

Supporting Information

Heterogenized Ni-doped zeolitic imidazolate framework guide efficient trapping and catalytic conversion toward polysulfides for greatly improved lithium-sulfur batteries

Yuxiang Yang,^a Zhenhua Wang,^{*ad} Taizhi Jiang,^b Chen Dong,^a Zhu Mao,^a Chengyi Lu,^{ac} Wang Sun,^{ad} and Kening Sun^{*ad}

^a *Beijing Key Laboratory for Chemical Power Source and Green Catalysis, School of Chemistry and Chemical Engineering, Beijing Institute of Technology, Beijing 100081, China. *Email: bitkeningsun@163.com, wangzh@bit.edu.cn*

^b *Department of Chemical Engineering, University of Texas at Austin, Austin, TX 78712, USA*

^c *Shaanxi Applied Physics and Chemistry Research Institute, Xi'an, Shaanxi 710061, China*

^d *Collaborative Innovation Center of Electric Vehicles in Beijing, Beijing 100081, China*

1. Experimental Section

1.1 Preparation of Ni-ZIF-8@CC and other control host materials

0.80 g zinc acetate (4.36 mmol), 0.1 g Ni(NO₃)₂·6H₂O (0.34 mmol), 2.00 g 2-methylimidazole and 0.40 g PEG (polyethylene glycol, Mn = 4000) were manually ground and mixed. The mixture was then loaded on a 4 cm × 4 cm carbon cloth, packed with aluminum foil and heated with electric iron at 200 °C for 10 min. After peeling off the aluminum foil, Ni-ZIF-8@CC was washed with ethanol, DMF, and water for several times. For the synthesis of Ni-ZIF-8@CC with different loadings of Ni-ZIF-8, we adjusted the weight of starting materials. After being treated under the same condition, Ni-ZIF-8@CC composites with different Ni-ZIF-8 loadings of 0.55, 0.76 and 1.05 mg cm⁻² (about 4.62 wt% Ni) were achieved, which were determined by elemental analyses. ZIF-8@CC was also prepared under the same condition except for the elimination of Ni(NO₃)₂·6H₂O.

1.2 Preparation of Ni-ZIF-8@CC/S and other control composites

To uniformly distribute sulfur in the Ni-ZIF-8@CC, 0.4 g of sulfur was dissolved in 10 mL of CS₂. Dry Ni-ZIF-8@CC composite was completely soaked in the CS₂ solution for 5 min, and then dried out at 45 °C for 12 h. Finally, the Ni-ZIF-8@CC/S composite was placed in an autoclave and heated at 155 °C for 12 h to obtain the Ni-ZIF-8@CC/S composite. The average sulfur mass loading is about 1.5 mg cm⁻², which was determined by the weight of the substrate before and after impregnation of sulfur. The thick electrode with a sulfur loading of 5.5 mg cm⁻² was prepared by adjusting the concentration of the S/CS₂ solution. Notably, the sulfur contents with

respect to the whole cathode, including the current collector, were about 10.0 and 29.0 wt% for the cathodes with 1.5 and 5.5 mg cm⁻², respectively. ZIF-8@CC/S and CC/S were also prepared under the same conditions for comparison.

1.3 Materials characterization

The morphologies were obtained using scanning electron microscopy (SEM, Quanta FEG 250) and transmission electron microscopy (TEM, JEOL JEM-2100F). STEM images and energy dispersive X-ray spectroscopy (EDX) elemental maps were obtained on a high angle annular dark field scanning transmission electron microscopy (HAADF-STEM, JEOL 2010F). Electrical properties were recorded by the use of a Keithley 4200 semiconductor characterization system (USA). The crystal structure of the samples was determined by X-ray powder diffraction (XRD, Rigaku Ultima IV, Cu-K α radiation, 40 kV, 50 mA). A plasma atomic emission spectroscopy (ICP-AES) was used to identify the elemental composition of the loading contents. The pore structure were characterized by nitrogen sorption using a Micrometrics ASAP 2020 physisorption analyzer. X-ray photoelectron spectroscopy (XPS) was carried out on Physical Electronics 5400 ESCA.

1.4 Electrochemical measurements

The Ni-ZIF-8@CC/S material was employed as the cathode without any polymer binder. CR-2025 type coin cells were assembled in a glove box filled with argon, using Li foil as the anode and a Celgard 2400 membrane as the separator. The electrolyte (purchased from Beijing Institute of Chemical Reagents) was 1.0 M lithium bis(trifluoromethanesulfonyl)imide (LiTFSI) dissolved in the DOL/DME

solvent (1:1 v/v) with 1 wt% LiNO₃ additives. An amount of 30 μ L and 80 μ L was applied in the cells with 1.5 and 5.5 mg cm⁻², respectively. The cells were charged and discharged on a battery test system (LAND CT2001A) between 1.8 and 2.8 V vs. Li⁺/Li. Specific capacity values were calculated according to the mass of sulfur. Electrochemical impedance spectroscopy (EIS) was measured by a PARSTAT 2273 at a frequency range from 100 kHz to 100 mHz with an AC voltage amplitude of 5 mV. Cyclic voltammetry measurements were performed on a CHI660D (Shanghai Chenhua Instrument) from 1.8 to 2.8 V with a scan rate from 0.1 to 0.5 mV s⁻¹.

1.5 The DFT calculation

The CASTEP module of Materials Studio software was used in the DFT calculations on structural and energy of all structures. The ultra-soft pseudopotentials were used to represent the interactions between the ionic cores and the valence electrons. The exchange-correlation functions were treated under the generalized gradient approximation (GGA). The plane-wave basis set cut-off energy was fixed at 400 eV in all calculations after convergence test. The special points sampling integration over Brillouin zone was conducted using the Monkhorst-Pack method with a 4 \times 4 \times 4 special k-points mesh. The geometry optimization was achieved under the Broyden-Fletcher-Goldfarb-Shanno minimization scheme. The crystal structures, including lattice constants and internal atomic coordinates, were optimized independently to minimize the free enthalpy, interatomic forces, and stresses of the unit cell. The tolerances for geometrical optimization were: differences for total energy within 10⁻⁵ eV/atom, maximum ionic Hellmann–Feynman force within 0.03

eV/Å, maximum ionic displacement within 0.001 Å, and maximum stress within 0.05

GPa. The calculated binding energies are defined as follows:

$$E_b = E_{s+sub} - (E_s + E_{sub})$$

where E_{s+sub} , E_s , and E_{sub} are the energy of the polysulfides-substrate, polysulfides, and substrate, respectively.

2. Supporting Figures

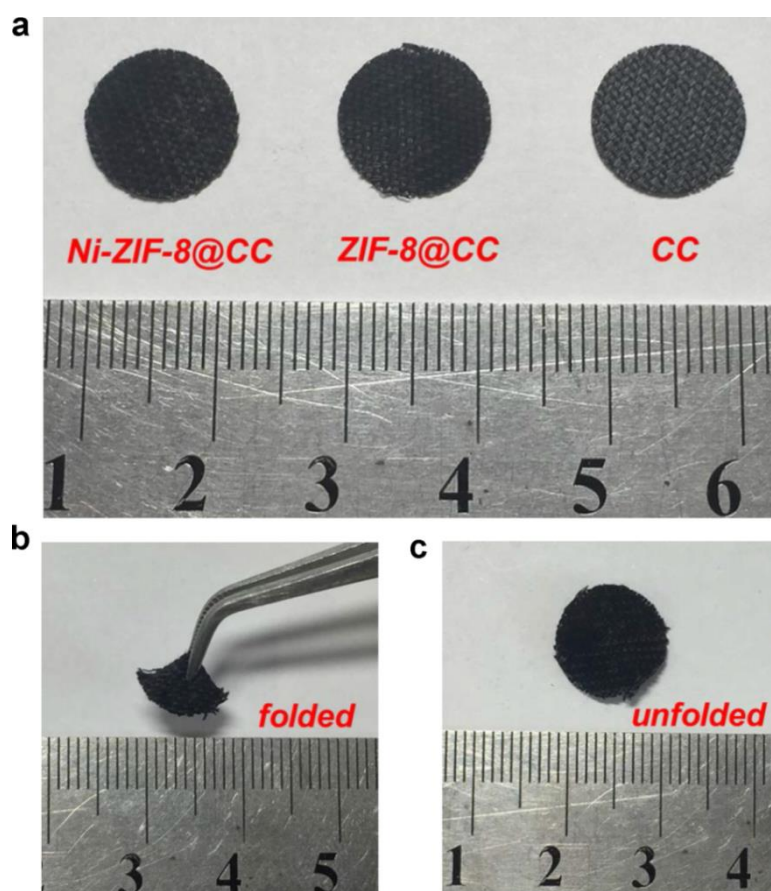


Fig. S1. (a) Photographs of the as-prepared Ni-ZIF-8@CC, ZIF-8@CC, and CC.

Photographs of the Ni-ZIF-8@CC (b) folded and (c) unfolded.

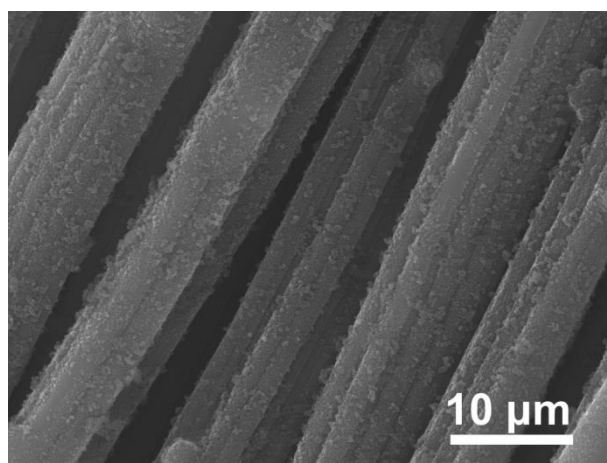


Fig. S2. Low magnification SEM image of the Ni-ZIF-8@CC.

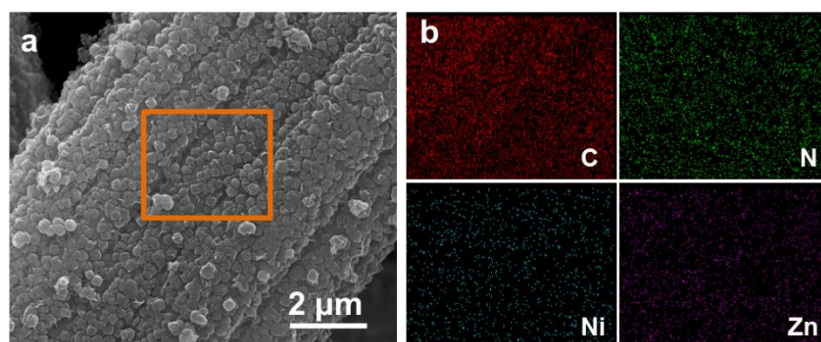


Fig. S3. (a) SEM image of the Ni-ZIF-8@CC composite with the optimized Ni-ZIF-8 loading of 7.66 mg cm^{-2} , and EDX elemental maps of (b) carbon, (c) nitrogen, (d) nickel and (e) zinc in the yellow solid line area, respectively.

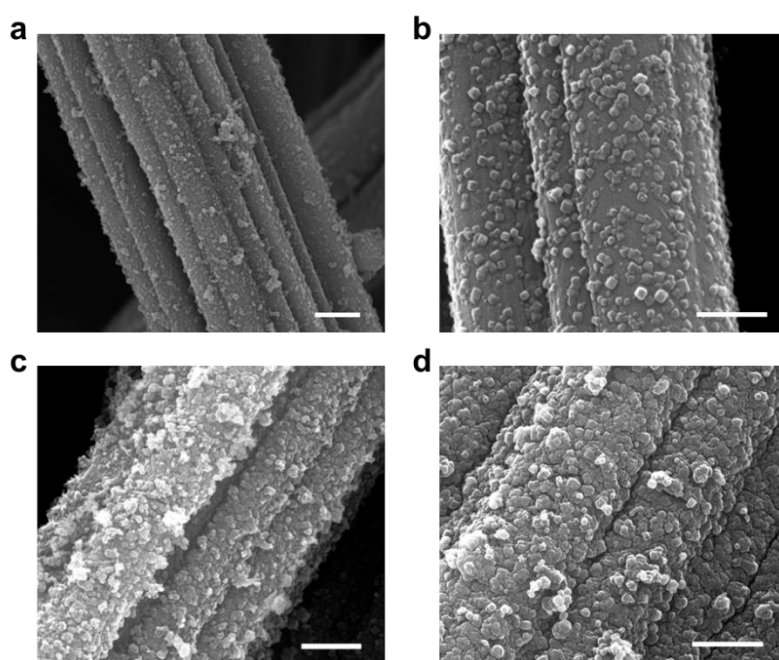


Fig. S4. (a,b) Ni-ZIF-8@CC with Ni-ZIF-8 loading of 5.50 g m^{-2} . (c,d) Ni-ZIF-8@CC with Ni-ZIF-8 loading of 10.50 g m^{-2} . Scale bars, (a,c) 2 μm ; (b,d) 1 μm .

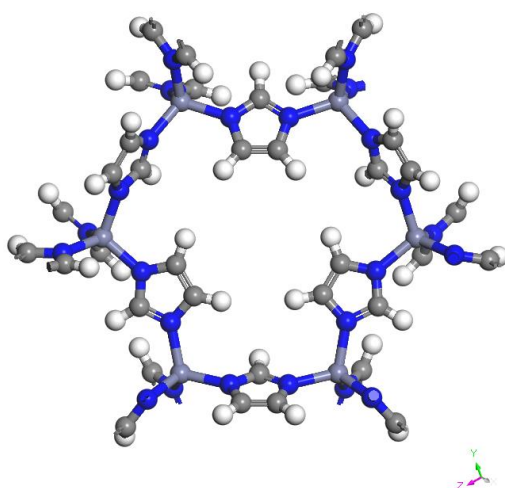


Fig. S5. Illustration of the structure of ZIF-8. Orchid, blue, gray and white spheres represent Zn, N, C and H atoms, respectively.

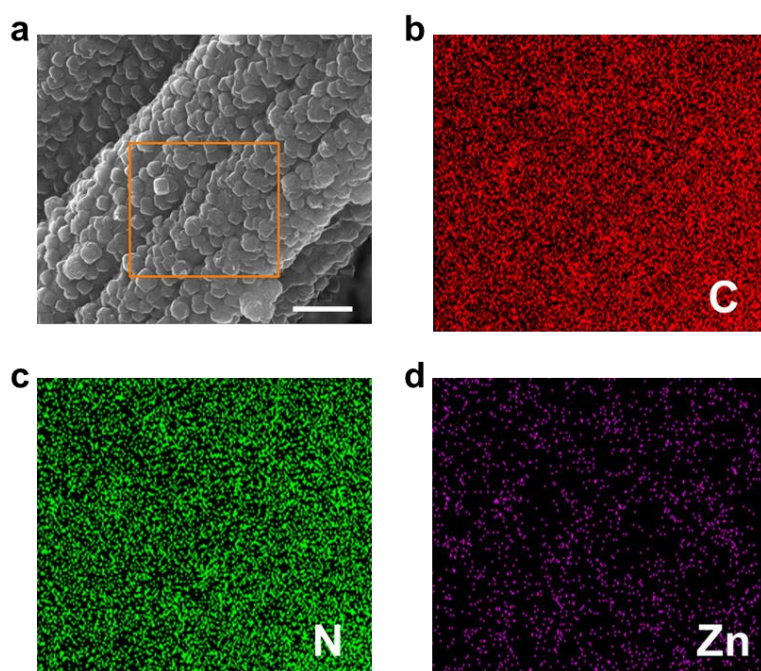


Fig. S6. (a) SEM image of the ZIF-8@CC composite, and EDX elemental maps of (b) carbon, (c) nitrogen and (d) zinc in the yellow solid line area, respectively. Scale bars, 2 μm .

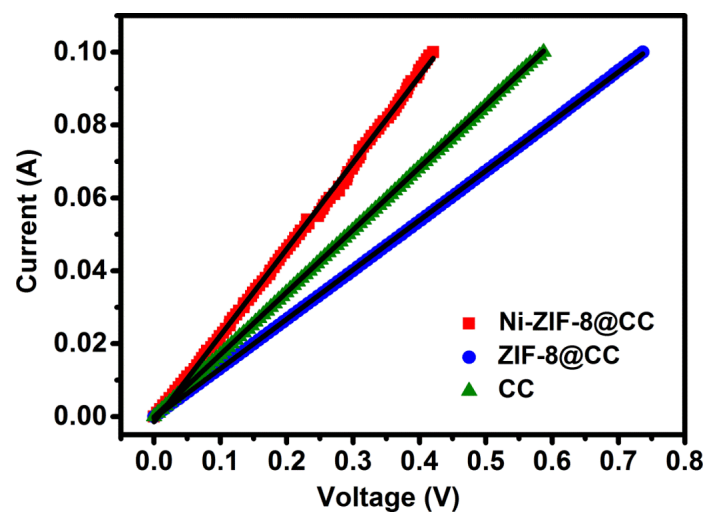


Fig. S7. I-V plots of Ni-ZIF-8@CC, ZIF-8@CC and CC composites.

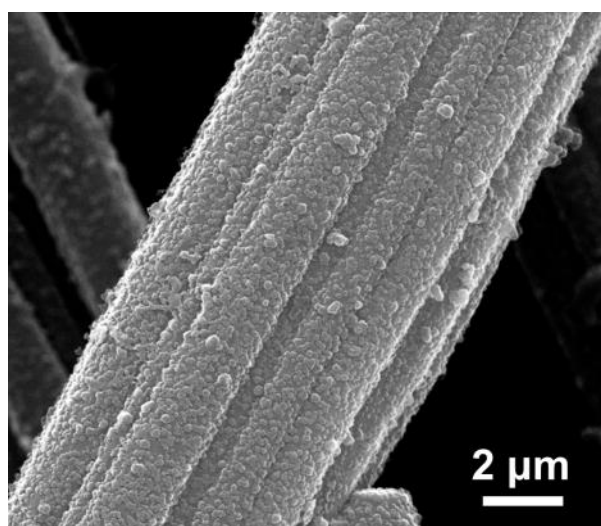


Fig. S8. SEM image of Ni-ZIF-8@CC/S.

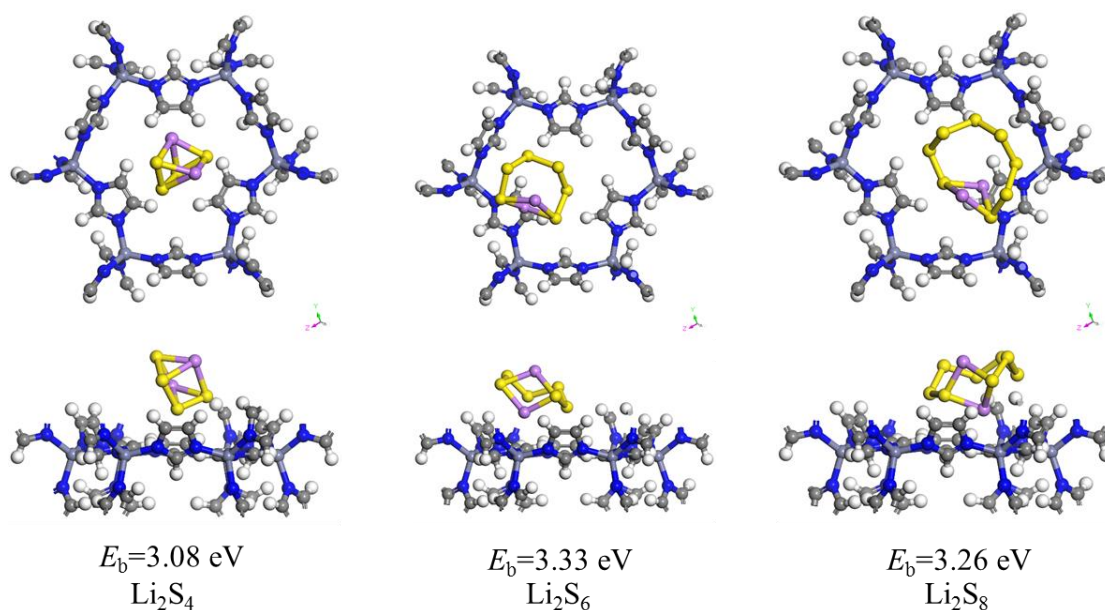


Fig. S9. Binding geometric configurations and binding energies of Li_2S_x ($x=4, 6$ and 8) species in pores of ZIF-8.

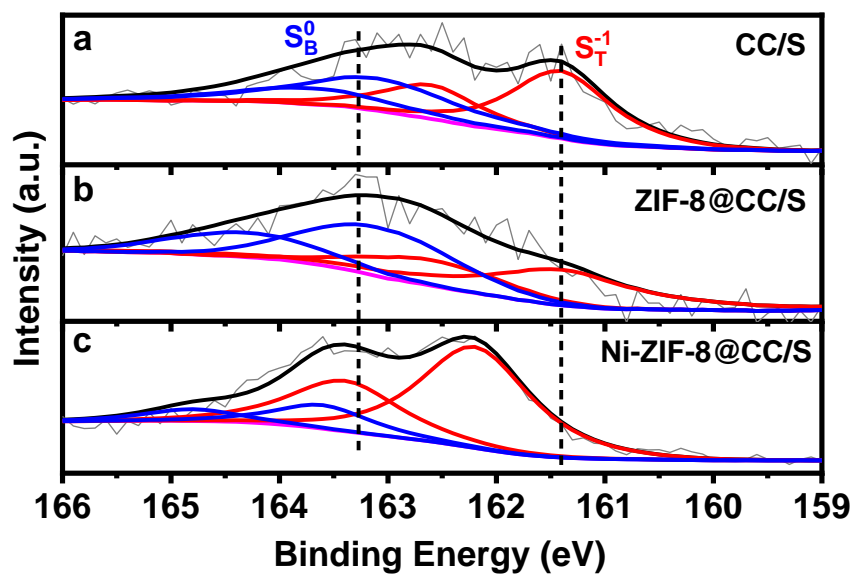


Fig. S10. XPS study of the interaction between polysulfide species and (a) CC/S, (b) ZIF-8@CC/S and (c) Ni-ZIF-8@CC/S cathodes after discharging to ~ 2.0 V.

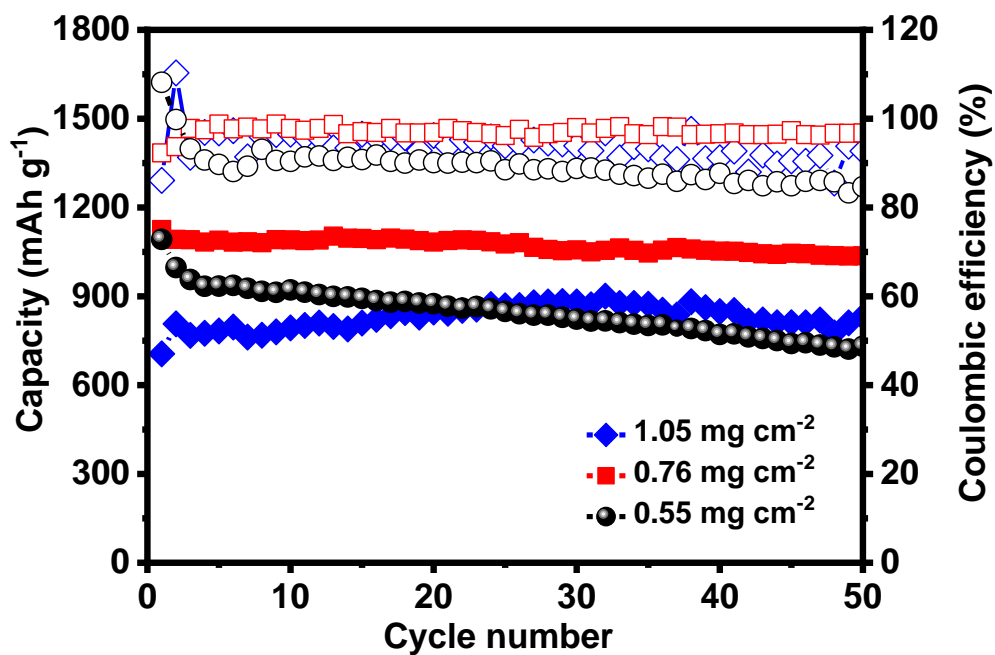


Fig. S11. Cycling performance of Ni-ZIF-8@CC/S electrodes with different loading of Ni-ZIF-8.

The cycling stability is improved with an appropriate increase in the content of Ni-ZIF-8 owing to enhanced confinement and cooperative catalysis for sulfur species, while the capacity is significantly limited due to poor electrode conductivity resulting from the excess loading (1.05 mg cm^{-2}). Therefore, the optimal loading of Ni-ZIF-8 here is 0.76 mg cm^{-2} , which exhibits the best cycling performance among the compared electrodes. The loading of ZIF-8 on CC is also optimized as above.

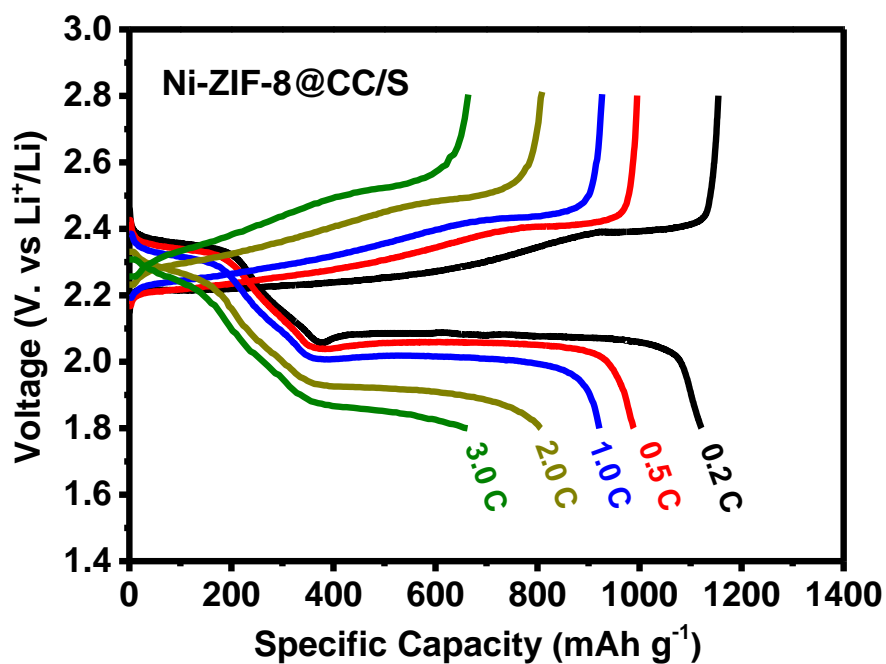


Fig. S12. Charge/discharge voltage profiles of Ni-ZIF-8@CC/S cathode performed at varied current rates.

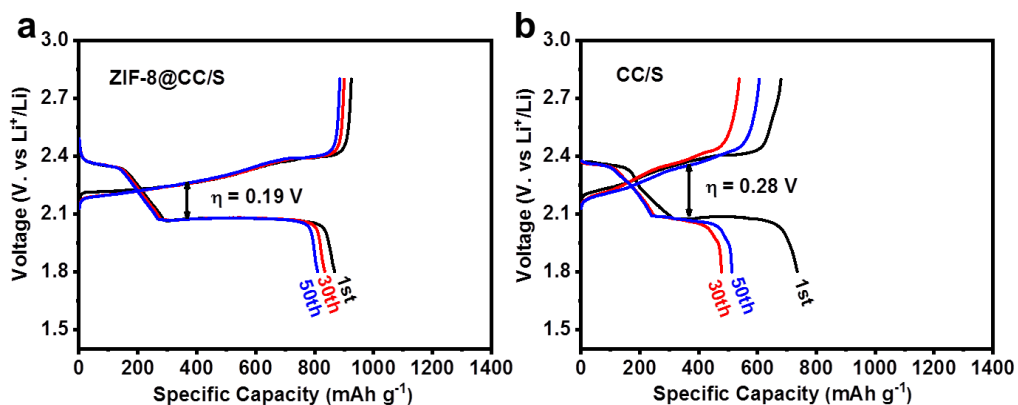


Fig. S13. Charge/discharge voltage profiles of (a) ZIF-8@CC/S and (b) CC/S cathodes at 0.2 C.

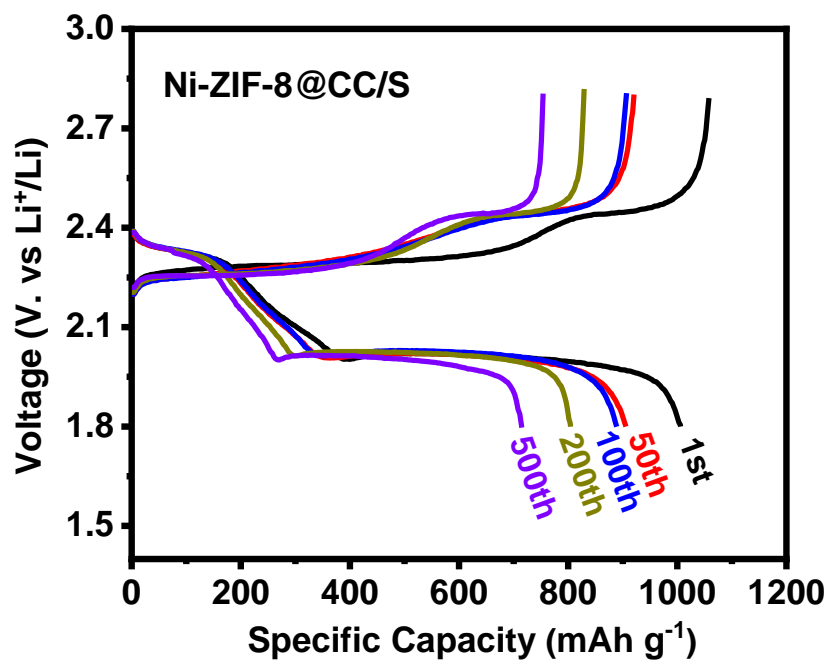


Fig. S14. Charge/discharge voltage profiles of Ni-ZIF-8@CC/S cathode at 1 C.

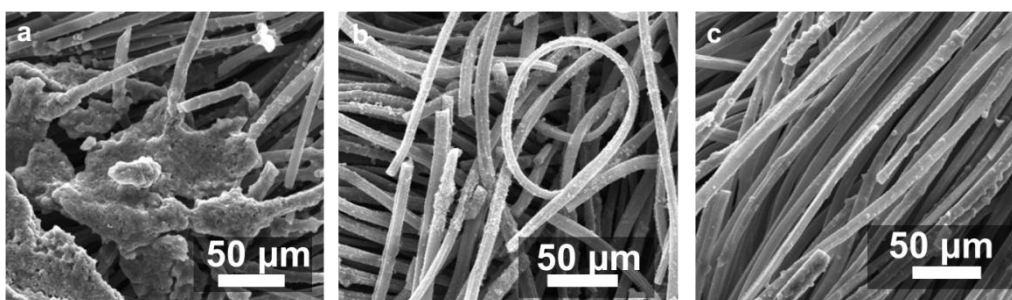


Fig. S15. Low magnification SEM images of the cycled (a) CC/S, (b) ZIF-8@CC/S, and (c) Ni-ZIF-8@CC/S electrodes.

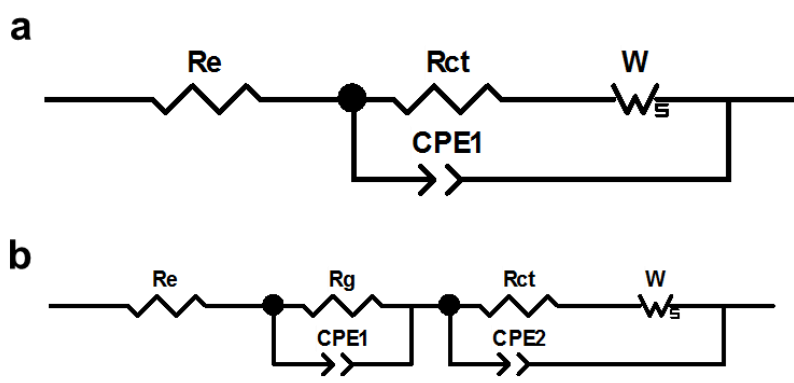


Fig. S16. The equivalent circuit for the fitting of the electrochemical impedance spectra (a) before and (b) after cycling.

Table S1. Comparisons of the lithium-ion diffusion coefficient (D_{Li^+}) of Li-S cells with different cathodes.

D_{Li^+} ($cm^2 s^{-1}$)	A (anodic peak at 2.5 V)	C1 (cathodic peak at 2.3 V)	C2 (cathodic peak at 2.0 V)
Ni-ZIF-8@CC/S	1.39×10^{-7}	3.67×10^{-8}	8.01×10^{-8}
ZIF-8@CC/S	1.06×10^{-7}	2.32×10^{-8}	5.83×10^{-8}
CC/S	7.32×10^{-8}	3.18×10^{-8}	2.41×10^{-8}

Table S2. The fitting results of the electrochemical impedance spectra of the fresh and cycled Ni-ZIF-8@CC/S, ZIF-8@CC/S, and CC/S electrodes.

	R_e / Ω	R_g / Ω	R_{ct} / Ω
Fresh Ni-ZIF-8@CC/S	2.041		20.48
Fresh ZIF-8@CC/S	1.652		18.94
Fresh CC/S	1.651		19.91
Cycled Ni-ZIF-8@CC/S	2.781	1.03	3.151
Cycled ZIF-8@CC/S	3.967	15.89	17.48
Cycled CC/S	4.354	45.3	88.93

Table S3. The performance comparisons of MOFs-based systems in lithium-sulfur electrodes.

MOF type	Areal sulfur loading/ mg cm ⁻²	Sulfur content (including the current collector ^a)	Initial discharge capacity/ mAh g ⁻¹	Discharge capacity after several cycles/ mAh g ⁻¹	Areal capacity/ mAh cm ⁻²
Ni-ZIF-8 (This work)	1.5	10.0%	1125	1036 after 50 cycles, 0.2 C	1.69
			1006	715 after 500 cycles, 1.0 C	1.51
	5.5	29.0%	1098	887 after 100 cycles, 1.2 mA cm ⁻²	6.04
MIL-100(Cr) ¹	-	10.0%	~1630	600 after 100 cycles, 0.1 C	-
HKUST-1/CNT ²	1.0	40.0%	1263	680 after 500 cycles, 0.2 C	1.26
	4.57		765	545 after 50 cycles, 0.2 C	3.59
MOF@GO ³	0.6-0.8	10.3%	1207	855 after 1500 cycles, 1.0 C	0.72-0.96
ZIF-8 ⁴	-	12.3%	738	654 after 100 cycles, 0.5 C	-
Ni ₆ (BTB) ₄ (BP) ₃ ⁵	-	14.6%	~617	~520 after 100 cycles, 0.2C	-
COF-1 ⁶	-	11.2%	1628	929 after 100 cycles, 0.2 C	-
			1032	770 after 200 cycles, 0.5 C	

^aThe weight of Al foil used in the literature is 4.736 mg cm⁻² (from the product datasheet on MTI Corporation), and the weight of CC current collector used here is about 12.8 mg cm⁻².

References

- 1 R. Demir-Cakan, M. Morcrette, F. Nouar, C. Davoisne, T. Devic, D. Gonbeau, R. Dominko, C. Serre, G. Ferey and J. M. Tarascon, *J. Am. Chem. Soc.*, 2011, **133**, 16154-16160.
- 2 Y. Mao, G. Li, Y. Guo, Z. Li, C. Liang, X. Peng and Z. Lin, *Nat. Commun.*, 2017, **8**, 14628.
- 3 S. Bai, X. Liu, K. Zhu, S. Wu and H. Zhou, *Nat. Energy*, 2016, **1**, 16094.
- 4 J. Zhou, R. Li, X. Fan, Y. Chen, R. Han, W. Li, J. Zheng, B. Wang and X. Li, *Energy Environ. Sci.*, 2014, **7**, 2715-2724.
- 5 J. Zheng, J. Tian, D. Wu, M. Gu, W. Xu, C. Wang, F. Gao, M. H. Engelhard, J. G. Zhang, J. Liu and J. Xiao, *Nano Lett.*, 2014, **14**, 2345-2352.
- 6 Z. A. Ghazi, L. Zhu, H. Wang, A. Naeem, A. M. Khattak, B. Liang, N. A. Khan, Z. Wei, L. Li and Z. Tang, *Adv. Energy Mater.*, 2016, **6**, 1601250.